SEISMIC IMPEDANCE AND POROSITY: SUPPORT EFFECTS

To be presented at Fifth International Geostatistics Congress, 22-27 September 1996, Wollongong, Australia

PETTER ABRAHAMSEN, ANNE-LISE HEKTOEN, LARS HOLDEN AND KRISTIN L. MUNTHE

Norwegian Computing Center
P.O. Box 114 Blindern
N-0314 Oslo, Norway

Abstract. A modification to the standard cokriging approach using impedance as a covariate to porosity is presented. To consider the inherent low vertical and lateral resolution of seismic data, the observed seismic impedance is assumed to be a noise corrupted version of the smoothed porosity field. Some approximations for efficient computing is also presented.

1. Introduction

The introduction of widely used 3-D seismic data and the increased quality of such data has boosted the attempts for using seismic data to improve reservoir characterization. The inherently low vertical and lateral resolution of such data makes the extracted parameters such as travel times and impedances uncertain. Moreover, the link to geological and petrophysical properties such as zone boundaries, facies distributions, and porosities, is not unique. However, the superior lateral coverage as opposed to well observations makes seismic data a valuable source of information.

Several suggestions to how seismic post-stack data can be utilized in reservoir characterization has been proposed. Most geostatistical attempts seek to find empirical correlations between a seismic parameter and porosity. The geostatistical attempts to utilize seismic data group into two major categories: Those using techniques related to cokriging and those using indicator kriging. Here we pursue the use of cokriging but relax the common

assumption of using the same correlation function for porosity and seismic parameter. The inherent smoothing effects of post-stack seismic data is considered explicitly so that the different support volumes for seismic data and porosity data are handled properly.

2. Position of the problem

2.1. SEISMIC PARAMETERS

The seismic parameters considered in the literature are, velocities (not stacking), travel times, amplitudes, and inverted impedances. All these parameters are to a certain extent linked to porosity. Using velocities or travel times however, implicitly requires that the thickness of the reservoir zone is known since otherwise varying travel time could be explained by varying thickness. Moreover, there is no direct physical link between amplitude at a certain location and porosity at the same location. Therefore, conditioning porosity directly on amplitude is questionable. This leaves us with inverted impedances which is difficult to obtain since the inversion process is ambiguous without imposing restrictions on the solution.

Seismic amplitudes are linked to reflection coefficients which is related to impedance contrasts. Seismic inversion or deconvolution of post-stack traces are used to extract impedance data from the traces. The result is 2-D impedance maps or 3-D impedance cubes. The impedance is the product of the pressure wave velocity and the density of the rock. The relation between velocity and density to porosity, is not unique and no simple relationship exist. Therefore most approaches take an empirical approach utilizing the statistical correlation found between seismic parameters and well observations of the rock parameter considered.

2.2. GEOSTATISTICAL METHODS

Several geostatistical methods for mapping porosities using seismic post-stack data have been applied:

Cokriging assumes that the seismic parameter is a covariate with its own stochastic properties. Covariance functions for the porosity field and the seismic parameters must be established and the cross-covariances between porosity and the seismic parameters must be obtained. There are severe restrictions on the relationship between these three covariance functions to guarantee a solution to the kriging system. Therefore, it is common to use the same correlation function for the porosity field and the seismic parameter. The cross-covariance function is then chosen to have the same form with an additional nugget effect.

Norwegian Computing Center, Box 114 Blindern, N-0314 Oslo, Norway, Tel.: (+47) 22 85 25 00

The first attempt to integrate seismic data (transit travel-time) and porosities from well logs within a cokriging framework is reported by Doyen (1988) and Western Geophysical Company (1988). Verly (1993) used normal score transformed impedances for porosity prediction. Burns, Cooper, den Boer, Doyen & Smart (1993) linked porosity directly to post-stack amplitudes using cokriging. Gorell (1995) applies sequential Gaussian simulation guided by synthetic velocities to obtain porosity maps.

A significant problem using cokriging is the enormous amount of seismic data entering the cokriging system. A simplified technique called *collocated cokriging* (Xu, Tran, Srivastava & Journel 1992) retains only the closest data. Collocated cokriging has been applied by Bashore, Araktingi, Levy & Schweller (1993) using impedances and Almeida, Tran & Balin (1993) using seismic velocities.

Universal kriging or 'kriging with a trend' uses a linear trend to establish the relationship between the seismic parameter and porosity. Araktingi, Bashore, Hewett & Tran (1990) compares universal kriging to indicator kriging with the Markov Bayes assumption. Chambers (1993) uses reflection amplitudes as an explanatory variable. Kjellesvik (1993) relates porosity to inverse impedance (Pickett 1963) using Bayesian kriging. Universal kriging with is closely related to cokriging conditioned on a dense grid of covariates.

Indicator kriging accepts any marginal distribution but requires a discretization of the continuous field. The porosity values are coded as indicators for a chosen set of threshold values. Simulation from the indicator kriging formalism is done using the SIS algorithm (Journel & Alabert 1990). Seismic information is coded as 'soft' indicators in the range [0,1] (Journel 1986). Thadani (1993) use this approach to relate amplitude data to porosities. The problem of estimating the variograms and co-variograms of the indicators are simplified by adopting the *Markov Bayes formalism* (Zhu & Journel 1993). The Markov Bayes approach has been used by Araktingi et al. (1990) and Araktingi & Bashore (1992) to obtain porosities from impedances.

3. Stochastic Models

3.1. POROSITY — $\Phi(\mathbf{x})$

The porosity is modeled as a Gaussian random field

$$\Phi(\mathbf{x}) = \mu_\Phi(\mathbf{x}) + \varepsilon_\Phi(\mathbf{x}), \qquad \mathbf{x} \in \mathbf{R}^3,$$

with expectation $\mathrm{E}\{\Phi(\mathbf{x})\} = \mu_\Phi(\mathbf{x})$ and covariances $\mathrm{Cov}\{\Phi(\mathbf{x}), \Phi(\mathbf{y})\} = \mathrm{Cov}\{\varepsilon_\Phi(\mathbf{x}), \varepsilon_\Phi(\mathbf{y})\} = \mathrm{C}_\Phi(\mathbf{x}, \mathbf{y})$.

Norwegian Computing Center, Box 114 Blindern, N-0314 Oslo, Norway, Tel.: (+47) 22 85 25 00

3.2. ACOUSTIC IMPEDANCE — $Z(\mathbf{x})$

The resolution of the seismics suggests that it is related to a smoothed version of the petrophysical field. The vertical resolution is limited by the seismic wavelength, and the lateral resolution is limited by the Fresnel zone, migration, and the stacking of CMP gathers.

Consider a smoothed version of $\Phi(\mathbf{x})$ defined by the convolution

$$\overline{\Phi}(\mathbf{x}) = w(\mathbf{x}) \star \Phi(\mathbf{x}) = \int_{\mathbf{R}^3} \Phi(\mathbf{t})\, w(\mathbf{x};\mathbf{t})\, d\mathbf{t}; \qquad \mathbf{x},\mathbf{t} \in \mathbf{R}^3,$$

where $\int_{\mathbf{R}^3} w(\mathbf{x})\, \mathrm{d}\mathbf{x} = s_0$ is a *scaling* factor.

The smoothed porosity, $\overline{\Phi}(\mathbf{x})$, is also a Gaussian random field with expectation and covariances

$$\begin{aligned}
\mathrm{E}\Big\{\overline{\Phi}(\mathbf{x})\Big\} &= \mu_{\overline{\Phi}}(\mathbf{x}) = w(\mathbf{x}) \star \mu_{\Phi}(\mathbf{x}), \\
\mathrm{Cov}\Big\{\overline{\Phi}(\mathbf{x}), \overline{\Phi}(\mathbf{y})\Big\} &= \mathrm{C}_{\overline{\Phi}}(\mathbf{x},\mathbf{y}) = w(\mathbf{x}) \star w(\mathbf{y}) \star \mathrm{C}_{\Phi}(\mathbf{x},\mathbf{y})\,, \\
\mathrm{Cov}\Big\{\overline{\Phi}(\mathbf{x}), \Phi(\mathbf{y})\Big\} &= \mathrm{C}_{\overline{\Phi}\Phi}(\mathbf{x},\mathbf{y}) = w(\mathbf{x}) \star \mathrm{C}_{\Phi}(\mathbf{x},\mathbf{y})\,.
\end{aligned}$$

Assume that the function $w(\cdot)$ can be chosen so the convolution resembles the real smoothing in seismics. Then the impedance, $Z(\mathbf{x})$, can be written:

$$Z(\mathbf{x}) = s_1 + \overline{\Phi}(\mathbf{x}) + \varepsilon_Z(\mathbf{x}); \qquad \mathbf{x} \in \mathbf{R}^3,$$

where the residual $\varepsilon_Z(\mathbf{x})$ is independent of $\Phi(\mathbf{x})$ and $\overline{\Phi}(\mathbf{x})$ and s_1 is a *shift* parameter. The residual is interpreted as zero mean noise and modeled as a Gaussian variable with covariances $\mathrm{Cov}\{\varepsilon_Z(\mathbf{x}), \varepsilon_Z(\mathbf{y})\} = \mathrm{C}_{\varepsilon_Z}(\mathbf{x},\mathbf{y})$. Then, $Z(\mathbf{x})$ will be a Gaussian random field with moments

$$\begin{aligned}
\mathrm{E}\{Z(\mathbf{x})\} &= \mu_Z(\mathbf{x}) = s_1 + w(\mathbf{x}) \star \mu_{\Phi}(\mathbf{x}), \\
\mathrm{Cov}\{Z(\mathbf{x}), Z(\mathbf{y})\} &= \mathrm{C}_Z(\mathbf{x},\mathbf{y}) = \mathrm{C}_{\overline{\Phi}}(\mathbf{x},\mathbf{y}) + \mathrm{C}_{\varepsilon_Z}(\mathbf{x},\mathbf{y})\,, \\
\mathrm{Cov}\{Z(\mathbf{x}), \Phi(\mathbf{y})\} &= \mathrm{C}_{\Phi Z}(\mathbf{x},\mathbf{y}) = \mathrm{C}_{\overline{\Phi}\Phi}(\mathbf{x},\mathbf{y})\,.
\end{aligned}$$

A stochastic model linking the petrophysical parameter, $\Phi(\mathbf{x})$, and the seismic parameter $Z(\mathbf{x})$ has been established. The strength of the link is determined by the variance of the seismic noise, $\varepsilon_Z(\mathbf{x})$ relative to the variance of $\overline{\Phi}(\mathbf{x})$.

4. Estimation

There are several parameters in the stochastic models which need to be estimated or specified. The scaling parameter, s_0, and the shift parameter,

Norwegian Computing Center, Box 114 Blindern, N-0314 Oslo, Norway, Tel.: (+47) 22 85 25 00

s_1, can be estimated by simple linear regression of Φ on Z. The shift parameter is the intercept while the scaling parameter is the slope. Spatial correlations should in principle be considered for optimal estimates but the difference is usually possible to ignore for large datasets.

The shape of the filter $w(\cdot)$ is difficult to estimate. Some tests using maximum likelihood estimation for the filter width failed to give unique answers. The shape of the filter must therefore be determined from geophysical knowledge.

The covariance function of $\Phi(\mathbf{x})$ must be estimated from bore-hole data while the covariance function of $Z(\mathbf{x})$ can be estimated from the impedances. A problem however, is that the covariance function of $Z(\mathbf{x})$ is assumed to consist of two parts, a contribution from $\overline{\Phi}(\mathbf{x})$, and a contribution from the residual noise $\varepsilon_Z(\mathbf{x})$. For a known smoothing filter and a given covariance function for $\Phi(\mathbf{x})$, an estimate for $\mathrm{C}_{\mathcal{E}_Z}(\mathbf{x},\mathbf{y})$ can be calculated as: $\widehat{\mathrm{C}}_{\mathcal{E}_Z}(\mathbf{x},\mathbf{y}) = \widehat{\mathrm{C}}_Z(\mathbf{x},\mathbf{y}) - \widehat{\mathrm{C}}_{\overline{\Phi}}(\mathbf{x},\mathbf{y})$. Some precautions to guarantee positive definiteness must be made.

5. Conditional fields

Consider the situation where the impedances are observed (inverted) in a dense grid. Denote these observations $\mathbf{Z} = \{Z(\mathbf{x}_1^Z), \dots Z(\mathbf{x}_{N_Z}^Z\}$ where $\mathbf{x}_i^Z \in \mathbf{R}^3$ for all i. Moreover porosities are measured along bore-holes in several wells. Denote these observations $\mathbf{\Phi} = \{\Phi(\mathbf{x}_1^\Phi), \dots \Phi(\mathbf{x}_{N_\Phi}^\Phi\}$ where $\mathbf{x}_j^\Phi \in \mathbf{R}^3$ for all j.

The porosity field, $\Phi(\mathbf{x})$, conditioned to both sets of observations is sought, i.e. $\Phi(\mathbf{x})|\mathbf{Z},\mathbf{\Phi}$. To obtain the conditional field, the set of observations may either be used simultaneously or sequentially using the equivalence

$$\Phi(\mathbf{x})|\mathbf{Z},\mathbf{\Phi} \equiv (\Phi(\mathbf{x})|\mathbf{Z})|(\mathbf{\Phi}|\mathbf{Z}). \tag{1}$$

Both alternatives are presented below.

5.1. SIMULTANEOUS CONDITIONING.

The porosity at $\mathbf{x}$ and the observations $\mathbf{\Phi}$ and $\mathbf{Z}$ belong by assumption to a common $1 + N_\Phi + N_Z$-dimensional Gaussian distribution:

$$\begin{bmatrix} \Phi(\mathbf{x}) \\ \mathbf{\Phi} \\ \mathbf{Z} \end{bmatrix} \sim N_{1+N_\Phi+N_Z}\left(\begin{bmatrix} \mu_\Phi(\mathbf{x}) \\ \boldsymbol{\mu}_\Phi \\ \boldsymbol{\mu}_Z \end{bmatrix}, \begin{bmatrix} \sigma_\Phi^2(\mathbf{x}) & \mathbf{k}'_\Phi(\mathbf{x}) & \mathbf{k}'_{\Phi Z}(\mathbf{x}) \\ \mathbf{k}_\Phi(\mathbf{x}) & \mathbf{K}_\Phi & \mathbf{K}'_{\Phi Z} \\ \mathbf{k}_{\Phi Z}(\mathbf{x}) & \mathbf{K}_{\Phi Z} & \mathbf{K}_Z \end{bmatrix} \right).$$

Covariances are given by the covariance functions C_Z, C_Φ, and $C_{\Phi Z}$. Standard formulas for conditional expectation and variance for multi-Gaussian

distributions provide

(2a)
$$\begin{aligned}\mathrm{E}\{\Phi(\mathbf{x})|\mathbf{\Phi}=\phi,\mathbf{Z}=\mathbf{z}\} &= \mu_{\Phi|\Phi,Z}(\mathbf{x}) \\ &= \mu_\Phi(\mathbf{x}) + \mathbf{k}'(\mathbf{x})\,\mathbf{K}^{-1}\begin{bmatrix}\phi-\boldsymbol{\mu}_\Phi\\ \mathbf{z}-\boldsymbol{\mu}_Z\end{bmatrix}\end{aligned}$$

(2b)
$$\mathrm{Var}\{\Phi(\mathbf{x})|\mathbf{Z},\mathbf{\Phi}\} = \sigma^2_{\Phi|\Phi,Z}(\mathbf{x}) = \sigma^2_\Phi(\mathbf{x}) - \mathbf{k}'(\mathbf{x})\,\mathbf{K}^{-1}\mathbf{k}(\mathbf{x}),$$

where
$$\mathbf{k}(\mathbf{x}) = \begin{bmatrix}\mathbf{k}_\Phi(\mathbf{x})\\ \mathbf{k}_{\Phi Z}(\mathbf{x})\end{bmatrix} \quad \text{and} \quad \mathbf{K} = \begin{bmatrix}\mathbf{K}_\Phi & \mathbf{K}'_{\Phi Z}\\ \mathbf{K}_{\Phi Z} & \mathbf{K}_Z\end{bmatrix}.$$

These are the predictor and prediction error for $\Phi(\mathbf{x})$ given the data. The problem however is the size of $\mathbf{K}$. For any realistic dataset, the size will be to large for inversion. Thus, some alternative approaches for approximating these equations are necessary.

5.2. SEQUENTIAL CONDITIONING

Instead of conditioning Φ on both sets of observations simultaneously, it is possible to do this in a two step approach based on Equivalence (1). First $\Phi(\mathbf{x})|\mathbf{Z}$ is considered. Again a multi-normally vector is constructed:

$$\begin{bmatrix}\Phi(\mathbf{x})\\ \mathbf{Z}\end{bmatrix} \sim N_{1+N_Z}\left(\begin{bmatrix}\mu_\Phi(\mathbf{x})\\ \boldsymbol{\mu}_Z\end{bmatrix}, \begin{bmatrix}\sigma^2_\Phi(\mathbf{x}) & \mathbf{k}'_{\Phi Z}(\mathbf{x})\\ \mathbf{k}_{\Phi Z}(\mathbf{x}) & \mathbf{K}_Z\end{bmatrix}\right).$$

The moments of the field $\Phi(x)|\mathbf{Z}$ are again given by standard formulas:

(3a)
$$\begin{aligned}\mathrm{E}\{\Phi(\mathbf{x})|\mathbf{Z}=\mathbf{z}\} &= \mu_{\Phi|Z}(\mathbf{x}) \\ &= \mu_\Phi(\mathbf{x}) + \mathbf{k}'_{\Phi Z}(\mathbf{x})\mathbf{K}_Z^{-1}\left[\mathbf{z}-\boldsymbol{\mu}_Z\right],\end{aligned}$$

(3b)
$$\begin{aligned}\mathrm{Var}\{\Phi(\mathbf{x})|\mathbf{Z}\} &= \sigma^2_{\Phi|Z}(\mathbf{x}) \\ &= \sigma^2_\Phi(\mathbf{x}) - \mathbf{k}'_{\Phi Z}(\mathbf{x})\mathbf{K}_Z^{-1}\mathbf{k}_{\Phi Z}(\mathbf{x}),\end{aligned}$$

(3c)
$$\begin{aligned}\mathrm{Cov}\{\Phi(\mathbf{x})|\mathbf{Z},\Phi(\mathbf{y})|\mathbf{Z}\} &= \mathrm{C}_{\Phi|\mathbf{Z}}(\mathbf{x},\mathbf{y}) \\ &= \mathrm{C}_\Phi(\mathbf{x},\mathbf{y}) - \mathbf{k}'_{\Phi Z}(\mathbf{y})\mathbf{K}_Z^{-1}\mathbf{k}_{\Phi Z}(\mathbf{x}).\end{aligned}$$

The observations of the porosity field are now introduced remembering (1). The moments are again found by considering the multi-normally distributed vector

$$\begin{bmatrix}\Phi(\mathbf{x})|\mathbf{Z}\\ \mathbf{\Phi}|\mathbf{Z}\end{bmatrix} \sim N_{1+N_\Phi}\left(\begin{bmatrix}\mu_{\Phi_Z}(\mathbf{x})\\ \boldsymbol{\mu}_{\Phi|Z}\end{bmatrix}, \begin{bmatrix}\sigma^2_{\Phi_Z}(\mathbf{x}) & \mathbf{k}'_{\Phi|Z}(\mathbf{x})\\ \mathbf{k}_{\Phi|Z}(\mathbf{x}) & \mathbf{K}_{\Phi|Z}\end{bmatrix}\right).$$

Norwegian Computing Center, Box 114 Blindern, N-0314 Oslo, Norway, Tel.: (+47) 22 85 25 00

The covariance of the field $\Phi(\mathbf{x})|\mathbf{Z}$ which is used in both $\mathbf{k}_{\Phi|Z}$ and $\mathbf{K}_{\Phi|Z}$ is given by (3c). The conditional moments are

(4a)
$$\begin{aligned}\mathrm{E}\{(\Phi(\mathbf{x})|(\mathbf{Z}))|(\mathbf{\Phi}|\mathbf{Z}) = \phi\} &= \mu_{\Phi|\Phi,Z}(\mathbf{x}) \\ &= \mu_{\Phi|Z}(\mathbf{x}) + \mathbf{k}'_{\Phi|Z}(\mathbf{x})\mathbf{K}^{-1}_{\Phi|Z}\left[\phi - \boldsymbol{\mu}_{\Phi|Z}\right],\end{aligned}$$

(4b)
$$\begin{aligned}\mathrm{Var}\{(\Phi(\mathbf{x})|\mathbf{Z})|(\mathbf{\Phi}|\mathbf{Z})\} &= \sigma^2_{\Phi|\Phi,Z}(\mathbf{x}) \\ &= \sigma^2_{\Phi|Z}(\mathbf{x}) - \mathbf{k}'_{\Phi|Z}(\mathbf{x})\mathbf{K}^{-1}_{\Phi|Z}\mathbf{k}_{\Phi|Z}(\mathbf{x}).\end{aligned}$$

Note that these moments are identical to (2a) and (2b).

The benefit of the sequential conditioning approach is that the two sources of data are introduced in two separate operations. This will be exploited below when we introduce several possible approximations to make computations feasible.

5.3. APPROXIMATIONS

Neither of the two algorithms to find $\Phi(\mathbf{x})|\mathbf{\Phi}, \mathbf{Z}$ are applicable because of the vast amount of observations which requires inversions of correspondingly large matrices. A straight forward approach is to use neighborhoods.

5.3.1. *Neighborhoods*

Since the seismic is observed in all the grid-nodes, N_Z is a very large number and $\mathbf{K}_Z$ in (3a) to (3c) will be a matrix too large to invert. A reasonable approximation is to condition $\Phi(\mathbf{x})$ to those observations within a window around $\mathbf{x}$. Note that the covariance matrix and residual observations vector become location dependent. For a stationary field however, the location dependence disappear and a significant reduction in computations is gained.

In the sequential algorithm, the covariances for the field $\Phi(\mathbf{x})|\mathbf{Z}$, given by (3c), are needed to evaluate $\mathbf{k}_{\Phi|Z}(\mathbf{x})$ and $\mathbf{K}_{\Phi|Z}$ in (4a) and (4b). Since two locations are involved, the union of the two neighborhoods must be used. This will give a variable sized matrix $\mathbf{K}_Z$. The next approximation is intended to remove this problem.

5.3.2. *Approximations to* $\mathrm{C}_{\Phi|\mathbf{Z}}(\mathbf{x}, \mathbf{y})$

Consider the general form of a covariance function:

(5)
$$\mathrm{C}_{\Phi|\mathbf{Z}}(\mathbf{x}, \mathbf{y}) = \sigma_{\Phi|\mathbf{Z}}(\mathbf{x})\sigma_{\Phi|\mathbf{Z}}(\mathbf{y})\rho_{\Phi|\mathbf{Z}}(\mathbf{x}, \mathbf{y}).$$

The expression for $\sigma_{\Phi|\mathbf{Z}}(\mathbf{x})$, given by (3b), can be approximated using a local neighborhood. The expression for $\rho_{\Phi|\mathbf{Z}}(\mathbf{x}, \mathbf{y})$ however, includes $K_{\Phi|Z}$ which requires the use of $C_{\Phi|Z}$ given by (3c). Since $C_{\Phi|Z}$ includes two locations the

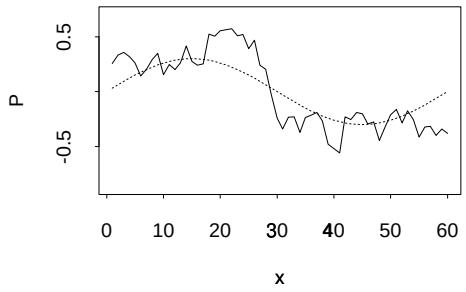

Figure 1. Cross section of porosity (solid line) with trend (dashed line).

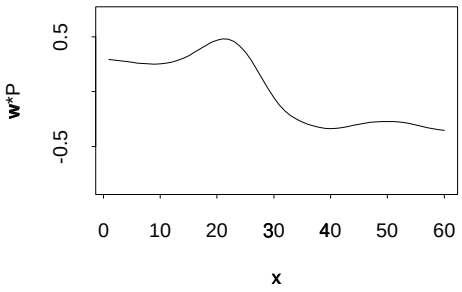

Figure 2. Cross section of smoothed porosity field. Smoothed version of solid line in Figure 1.

union of two neighborhoods must be considered and the size of K_Z in (3c) will depend on the two locations. To circumvent this problem $\rho_{\Phi|\mathbf{Z}}(\mathbf{x},\mathbf{y})$ is approximated by $\rho_\Phi(\mathbf{x},\mathbf{y})$ in (5):

$$\mathrm{C}_{\Phi|\mathbf{Z}}(\mathbf{x},\mathbf{y}) \approx \sigma_{\Phi|Z}(\mathbf{x})\sigma_{\Phi|Z}(\mathbf{y})\rho_\Phi(\mathbf{x},\mathbf{y}). \tag{6}$$

Thus, local neighborhoods can be applied without considering variable sized $\mathbf{K}_Z$ matrices.

5.3.3. *Summary of approximations*
The approximation of Equations (2a) and (2b) is done in the following steps:

1. Calculate $\mu_{\Phi|Z}(\mathbf{x})$ and $\sigma^2_{\Phi|Z}(\mathbf{x})$ using the local neighborhood approximations for $\mathbf{k}_{\Phi\mathbf{Z}}(\mathbf{x})$ and $\mathbf{K}_\mathbf{Z}$ in (3a) and (3b).
2. Calculate $\mu_{\Phi|\Phi,Z}(\mathbf{x})$ and $\sigma^2_{\Phi|\Phi,Z}(\mathbf{x})$ using $\mu_{\Phi|Z}(\mathbf{x})$ and $\sigma^2_{\Phi|Z}(\mathbf{x})$ and the approximation (6) in (4a) and (4b).

6. Examples

To demonstrate the properties of the convolution and the approximation a one dimensional example is given. The solid line in Figure 1 illustrates a cross-section of the porosity (arbitrary units). The dashed line is the trend, μ_Φ. By smoothing the porosity using a triangular filter with half-width 10, the smooth curve in Figure 2 appears.

6.1. DECONVOLUTION

First assume that ε_Z vanish, that is, the impedance is a pure convolution of the porosity. The predictor $\mathrm{E}\{\Phi(\mathbf{x})|\mathbf{Z}=\mathbf{z}\}$ given by (3a) is illustrated in Figure 3 as a solid line whereas the true porosity from Figure 1 is shown

Norwegian Computing Center, Box 114 Blindern, N-0314 Oslo, Norway, Tel.: (+47) 22 85 25 00

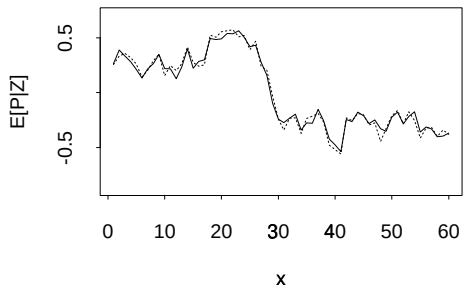

Figure 3. Deconvolution of smoothed porosity; Cross section of deconvolved porosity from Figure 2 (solid line) compared to 'true' porosity from Figure 1 (dashed line).

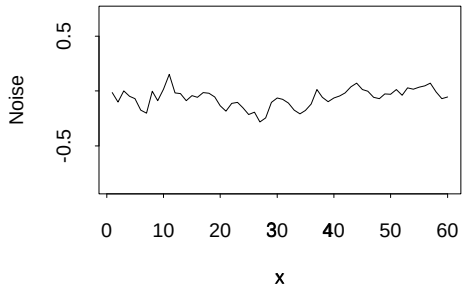

Figure 4. Cross section of seismic noise, $\mathcal{E}_Z$.

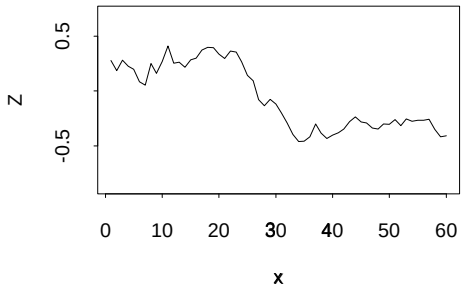

Figure 5. Cross section of impedance, $Z = \overline{\Phi} + \mathcal{E}_Z$.

as a dashed line. The predictor is a deconvolution of the smooth curve given in Figure 2. It is seen that the predictor (3a) gives a very detailed and accurate description of the porosity. This is of course not a realistic situation but it illustrates the deconvolution properties of cokriging with a smoothed covariate. When introducing noise in the seismic observations the situation changes. There becomes a competition between the deconvolution to exaggerate small fluctuations, and averaging to reduce noise.

6.2. CONSEQUENCE OF APPROXIMATION OF CORRELATION FUNCTION

Figure 4 is a cross section of the seismic noise $\mathcal{E}_Z$. By assumption the impedance, illustrated in Figure 5, is obtained by adding this noise to $\overline{\Phi}$ in Figure 2. Three porosity data locations have been selected. These are marked by a small dot in the following figures. Four different predictors and prediction errors are compared:

1. Conditioning on porosity data alone; see Figure 6.

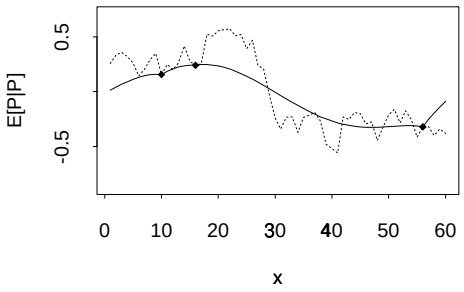

Figure 6. Cross section of porosity prediction conditioned on porosity data (solid line). 'True' porosity (dashed line).

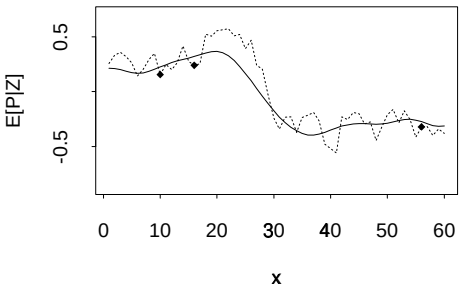

Figure 7. Cross section of porosity prediction conditioned on impedance data (solid line). 'True' porosity (dashed line).

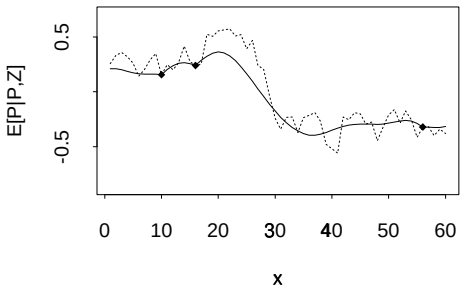

Figure 8. Cross section of porosity prediction conditioned on porosity and impedance data (solid line). 'True' porosity (dashed line).

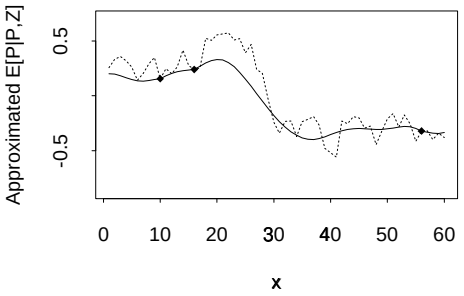

Figure 9. Cross section of porosity prediction conditioned on porosity and impedance data using approximation (6) (solid line). 'True' porosity (dashed line).

2. Conditioning on impedance data alone using (3a) and (3b); see Figure 7.
3. Conditioning on all data using the exact expressions (2a) and (2b); see Figure 8.
4. Conditioning on all data using (4a) and (4b) with approximation (6) for $C_{\Phi|\mathbf{Z}}(\mathbf{x}, \mathbf{y})$; see Figure 9.

The figures shows that using approximation (6) has minor influence on the predictor.

Figure 10 contains prediction errors for Cases 1. and 2., whereas Figure 11 contains prediction errors for Cases 3. and 4., The solid line in Figure 11 is the correct prediction error when using both sources of data. The dashed line, obtained using approximation (6), shows a to large influence form the porosity observations. The introduction of densely sampled impedance data screens the influence of point observations and this effect is ignored in the approximation.

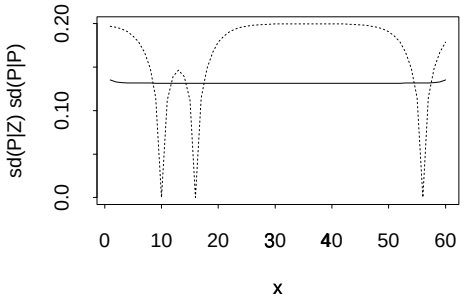

Figure 10. Cross section of prediction errors. Solid line is conditioned on impedance data alone. Dashed line is conditioned on porosity data.

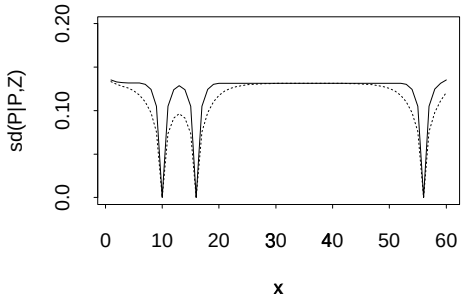

Figure 11. Cross section of prediction errors conditioned on both impedance and porosity data. Dashed line obtained by using (4b) with approximation (6).

7. Closing remarks

A modification to the standard cokriging approach to using impedance data for improving prediction of porosities has been developed. The difference to previous techniques is the introduction of a smoothing filter so that the inherent poor lateral and vertical resolution of the seismic signal can be handled properly.

Moreover, a two step approach for prediction has been introduced to speed up calculations. First, the expectation and variance of the porosity field given impedance data is calculated. Finally data from the porosity field itself is introduced. To simplify the calculations in the final step an approximation to the spatial correlation function is introduced. This approximation has minor influence on predictions, but prediction error becomes to small.

Acknowledgements

The work was supported by The Research Council of Norway.

References

Almeida, A. S., Tran, T. & Balin, P. R. (1993), An integrated approach to reservoir studies using stochastic simulation techniques, *in* Soares (1993), pp. 371–383.

Araktingi, U. G. & Bashore, W. M. (1992), Effects of properties in seismic data on reservoir characterization and consequent fluid-flow predictions when integrated with well logs, *in* SPE (1992), pp. 913–926. SPE 24752.

Araktingi, U. G., Bashore, W. M., Hewett, T. A. & Tran, T. T. B. (1990), Integration of seismic and well log data in reservoir modelling, *in* '3rd Annual NIPER Conference on Reservoir Characterization', Tulsa.

Bashore, W. M., Araktingi, U. G., Levy, M. & Schweller, W. J. (1993), The importance of the geological model for reservoir characterization using geostatistical techniques and the impact of subsequent fluid flow, *in* '68th Annual Technical Conference and

Exhibition', Society of Petroleum Engineers, Houston, Texas, pp. 601–616. SPE 26474.

Bortoli, L.-J., Alabert, F., Haas, A. & Journel, A. (1993), Constraining stochastic images to seismic data: Stochastic simulation of synthetic seismograms, *in* Soares (1993), pp. 325–337.

Burns, C. S., Cooper, D., den Boer, L., Doyen, P. & Smart, T. (1993), Reservoir characterization by seismically constrained stochastic simulation, *in* 'SPE Middle East Oil Technical Conference and Exhibition', Society of Petroleum Engineers, Bahrain, p. 8. SPE 25656.

Chambers, R. L. (1993), Geostatistical application for exploration and development: Porosity estimation from 3-D seismic data calibrated to well data, *in* '8th Annual Middle East Oil Show', Society of Petroleum Engineers, Bahrain, pp. 481–490. SPE 25655.

Doyen, P. M. (1988), 'Porosity from seismic data: A geostatistical approach', *Geophysics* **53**(10), 1263–1275.

Gorell, S. H. (1995), 'Using geostatistics to aid in reservoir characterization', *The Leading Edge* **14**(9), 967–974.

Haas, A. & Dubrule, O. (1994), 'Geostatistical inversion - a sequential method of stochastic reservoir modeling constrained by seismic data', *First Break* **12**(11), 561–569.

Journel, A. G. (1986), 'Constrained interpolation and qualitative information—the soft kriging approach', *Math. Geol.* **18**(3), 269–286.

Journel, A. G. & Alabert, F. G. (1990), 'New method for reservoir mapping', *JPT* **42**(2), 212–218.

Kjellesvik, L. E. (1993), Stochastic description of reservoir characteristics conditioned on seismic data, Diploma, Norwegian Institute of Technology, Trondheim, Norway.

Pickett, G. R. (1963), 'Acoustic character logs and their applications in formation evaluation', *JPT* pp. 659–667.

Soares, A., ed. (1993), *Geostatistics Tróia '92*, proc. '4th Inter. Geostat. Congr.', Tróia Portugal, 1992, Kluwer Academic Publishers, Dordrecht, 1088 pp.

SPE (1992), *67th Annual Technical Conference and Exhibition*, Wahington DC, Society of Petroleum Engineers.

Thadani, S. G. (1993), Reservoir characterization with seismic data using pattern recognition and spatial statistics, *in* Soares (1993), pp. 519–542.

Verly, G. W. (1993), Sequential Gaussian cosimulation: A simulation method integrating several types of information, *in* Soares (1993), pp. 543–554.

Western Geophysical Company (1988), Seismically enhanced reservoir characterization: An integrated geostatistical approach, Technical report, Western Atlas International, P.O.Box 2469, Houston, TX 77252, 30 pp.

Xu, W., Tran, T. T., Srivastava, R. M. & Journel, A. G. (1992), Integrating seismic data in reservoir modeling: The collocated cokriging alternative, *in* SPE (1992), pp. 833–842. SPE 24742.

Zhu, H. & Journel, A. G. (1993), Formatting and integrating soft data: Stochastic imaging via the Markov-Bayes algorithm, *in* Soares (1993), pp. 1–12.

Norwegian Computing Center, Box 114 Blindern, N-0314 Oslo, Norway, Tel.: (+47) 22 85 25 00